Journal of Marine Science and Technology

Volume 18 | Issue 6 Article 10

THE STUDY ON THE ASYMPTOTIC PROFILE AND THE FLOW PATTERNS IN FRONT OF A LONG BUBBLE THROUGH A CIRCULAR TUBE

Cheng-Hsing Hsu
Department of Mechanical Engineering, Chung-Yuan Christian University, Chung-Li 32023, Taiwan, R.O.C

Chia-Chuan Kuo
Department of Mechanical Engineering, Chung-Yuan Christian University, Chung-Li 32023, Taiwan, R.O.C, issackuo2007@gmail.com

Ching-Chuan Chang
Department of Mechanical Engineering, Chung-Yuan Christian University, Chung-Li 32023, Taiwan, R.O.C

Kuang-Yuan Kung
Department of Mechanical Engineering, Nanya Institute of Technology, Chung-Li 320, Taiwan, R.O.C

Recommended Citation

Hsu, Cheng-Hsing; Kuo, Chia-Chuan; Chang, Ching-Chuan; and Kung, Kuang-Yuan (2010) "THE STUDY ON THE ASYMPTOTIC PROFILE AND THE FLOW PATTERNS IN FRONT OF A LONG BUBBLE THROUGH A CIRCULAR TUBE," *Journal of Marine Science and Technology*: Vol. 18 : Iss. 6 , Article 10.
DOI: 10.51400/2709-6998.1944
Available at: https://jmstt.ntou.edu.tw/journal/vol18/iss6/10

Journal of Marine Science and Technology, Vol. 18, No. 6, pp. 860-866 (2010)

THE STUDY ON THE ASYMPTOTIC PROFILE AND THE FLOW PATTERNS IN FRONT OF A LONG BUBBLE THROUGH A CIRCULAR TUBE

Cheng-Hsing Hsu*, Chia-Chuan Kuo*, Ching-Chuan Chang*, and Kuang-Yuan Kung**

Key words: bubble, interface, flow patterns, stagnation point.

ABSTRACT

In this paper, the penetration of a long bubble through a Newtonian fluid in a horizontal circular tube is studied by numerical simulation. We simulate the evolution of the asymptotic bubble profiles with an interface-tracking method by conservative level set method.

The ratio of the asymptotic bubble width to the radius of the circular tube, i.e. λ, dominates not only the type of the flow patterns but also the location of the stagnation point. Three flow patterns suggested by Taylor in front of the bubble, namely the complete bypass flow, the transient flow and the recirculation flow are shown graphically. They make a good agreement with the study of Giavedoni and Hsu respectively. The stagnation point moves downstream as λ increases. The stagnation point moves here downstream with an almost constant rate of λ while $0.72 \leqq \lambda \leqq 0.9$.

I. INTRODUCTION

Many researchers have been involved in the study of the displacing of liquid expelled by gas. A variety of practical applications have been developed such as gas-assisted injection molding [11], fluidized bed [23], and two-phase flow in micro tubes [4].

From the beginning of the early bubble studies, the shape of the bubble is very attractive to the researchers. A shape profile equation, as the water penetrated the oil in a Hele-Shaw cell, was published by Saffman & Taylor (1958) [18]. They also defined the ratio λ as the fraction of the channel was occupied by the bubble. The bubble profile agreed very well with their shape equation only when $\lambda = 0.5$.

Paper submitted 08/06/09; revised 10/23/09; accepted 11/05/09. Author for correspondence: Chia-Chuan Kuo (e-mail: issackuo2007@gmail.com).
**Department of Mechanical Engineering, Chung-Yuan Christian University, Chung-Li 32023, Taiwan, R.O.C.*
***Department of Mechanical Engineering, Nanya Institute of Technology, Chung-Li 320, Taiwan, R.O.C.*

Later, a modified shape equation of the bubble front was proposed by Pitts (1980) [16] shown as Eq. (1). It agreed very well with the bubble profile observed as $\lambda = 0.54, 0.67, 0.77$.

$$\exp\left(\frac{\pi x}{2\lambda}\right)\cos\left(\frac{\pi y}{2\lambda}\right)=1 \tag{1}$$

where x, y are the Cartesian coordinates of the bubble profile.

By comparing their observing results with the work of Pitts, a formula for the axisymmetric case was proposed by Hsu [9]. They observed the bubble profile passing through the silicon oil in a circular tube experimentally by CCD camera and some image process procedures such as binarization and thinning etc.

Three flow patterns were suggested by Taylor [21]: two kinds of recirculating flows with a low capillary number and bypass flow with a high capillary number. Huzyak and Koelling [10] observed the bubble profile in a circular tube experimentally by CCD camera. Gauri and Koelling [5] measured the flow field near the bubble tip using the Particle Tracking Velocimetry (PTV) technique and presented the two typical flow patterns suggested by Taylor [21]. Zhong *et al*. [23] observed the flow patterns and transitions in a rectangular spout-fluid bed by a high-resolution digital CCD camera.

Some researchers simulated the formation of bubbles by numerical methods. The volume of fraction method (VOF) [7] and the level set method (LS) [19] are two most popular interface tracking methods used in multi-phase problem simulations.

Tomiyama [22] simulated a two-dimensional single bubble in a stagnant liquid and in a linear shear flow, which were conducted in the present study using the volume of fluid method.

Osher and Sethian [15] devised the level set algorithms based on Hamilton-Jacobi to tracking moving interfaces of the multi-phase flow. It is very powerful to deal with the shape and the normal. In many implementations, it was even very excellent to deal with the shape and normal of the geometry. However, the level set method was found to be a very large consumption of computer resources. Adalsteinsson [1] presented a fast level set method for propagating interfaces by using only points close to the curve at every time step to im-

prove the computation efficiency of the standard level set method. Nagrath *et al*. [13] simulated the incompressible bubble dynamics with a stabilized finite element level set method.

The level set technique is powerful in the automatic handling of topological changes, but it is poor at the mass conservation of the fluid [12]. The volume of fluid method conserves the mass exactly, but it is limited by its complexity of the reconstruction procedure [2]. Many researchers made much efforts to improve these disadvantages, e.g. Sussman *et al.* [20] showed a method by combining the advantages of the volume-of-fluid method with the level set method. Olsson and Kreiss [14] described the conservative level set method, which combines the merits of the volume-of-fluid method with the level set method. Bonometti and Magnaudet [2] presented an interface-capturing method borrowing some features from the volume of fluid method as well as from the level set technique.

Some researchers also simulated the flow field solving the Stokes equations by numerical methods. Giavedoni and Saita [9] simulated the interfacial shape and flow in front of a long bubble by the finite element method.

Polynkin *et al*. [17] simulated the flow patterns ahead of the gas bubble by using the finite element method. Hsu *et al.* [8] showed ranges of the three flow patterns suggested by Taylor [21] in 1961 by using a finite difference method (FDM) with successive over-relaxation (SOR).

In this paper, we aim to study the penetration of a long bubble through a Newtonian fluid in a circular tube by numerical simulation. The Navier-Stokes equations are used neglecting the inertial forces effects. The type of the flow patterns and the location of the stagnation point are solved by the finite difference method.

In stead of using an empirical deduced bubble profile formula in [8], our interface information is generated by an interface-tracking method. The evolution of the interface is performed by the conservative level set method [14]. Unlike other researchers focus on the study of smaller bubbles ($\lambda \leqq 0.8$), we focus on the bigger bubbles with the range of $0.7 \leqq \lambda \leqq 0.9$ in a lower speed $0 \leqq \mathrm{Re} \leqq 400$.

II. MODEL FORMULATION

1. Model Representation

A circular tube with radius R, is filled with viscous fluid. Air is injected into the tube from the entrance located on the left end of the tube. A long bubble is formed as the air steadily expels the viscous fluid. The model schematic drawing is shown in Fig. 1. As an axial-symmetrical problem, $\overline{\mathrm{FC}}$ is the symmetrical axis of the circular tube. $\overline{\mathrm{DE}}$ is the bubble front profile, i.e. the interface of the air and fluid, and $R = \overline{\mathrm{EF}}$ is the radius of the bubble. $\overline{\mathrm{FC}} = 6R$, $\overline{\mathrm{FD}} = 3R$, $\overline{\mathrm{DC}} = 3R$ and Hagen–Poiseuille law are obeyed in the far downstream $\overline{\mathrm{BC}}$ and the far upstream $\overline{\mathrm{AE}}$ [3]. The bubble elongates steadily

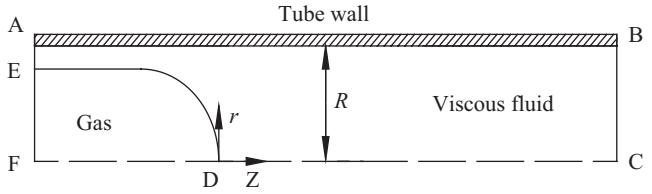

Fig. 1. The schematic of bubble and coordinates.

to the right with a constant velocity U, and the origin locates on the tip of the bubble front, i.e. point D. As a dynamic coordinates system, the coordinates system also moves steadily with the same velocity U to the right. The ratio λ is defined as the ratio of the asymptotic bubble width to the radius of the circular tube, i.e. $\lambda = \dfrac{\overline{\mathrm{EF}}}{\overline{\mathrm{BC}}}$.

2. Governing Equations

The axisymmetric equations of momentum are expressed as:

$$\begin{cases} u_r \dfrac{\partial u_r}{\partial r} + u_z \dfrac{\partial u_r}{\partial z} = -\dfrac{1}{\rho}\dfrac{\partial p}{\partial r} + \upsilon\left(\dfrac{1}{r}\dfrac{\partial}{\partial r}\left(r\dfrac{\partial u_r}{\partial r}\right) + \dfrac{\partial^2 u_r}{\partial z^2} - \dfrac{u_r}{r^2}\right) \\ u_r \dfrac{\partial u_z}{\partial r} + u_z \dfrac{\partial u_z}{\partial z} = -\dfrac{1}{\rho}\dfrac{\partial p}{\partial z} + \upsilon\left(\dfrac{1}{r}\dfrac{\partial}{\partial r}\left(r\dfrac{\partial u_z}{\partial r}\right) + \dfrac{\partial^2 u_z}{\partial z^2}\right) \end{cases} \tag{2}$$

The boundary conditions are:

1. Both the gas and liquid fit the continuity equation and are incompressible fluids with finite velocity.

$$\frac{1}{r}\frac{\partial (r u_r)}{\partial r} + \frac{\partial u_z}{\partial z} = 0 \tag{3}$$

where $\vec{u}$ is the velocity of the fluid, and u_r and u_z are the velocity components along r and z.

2. No-slip condition is assumed on the wall of the tube.

$$r = R, \quad -3R \le z \le 3R, \quad \vec{u} = 0 \tag{4}$$

3. Neglect the effect of gravity.
4. A fully developed flow assumption is made at the far upstream [3].

$$0 < r < R, \quad z = -3R, \quad v_r = 0, \quad \frac{\partial u_z}{\partial z} = 0 \tag{5}$$

5. Similarly, a fully developed flow assumption is made at the far downstream.

$$0 < r < R, \quad z = 3R, \quad v_r = 0, \quad \frac{\partial u_z}{\partial z} = 0 \tag{6}$$

6. The axial symmetry condition is considered on the symmetrical axis.

$$\frac{\partial}{\partial \theta} = 0, \quad r = 0, \quad -3R \le z \le 3R, \quad v_r = 0, \quad \frac{\partial u_z}{\partial r} = 0 \tag{7}$$

7. The evolution of the interface is expressed in the conservation form of the level set function

$$\frac{d\varphi}{dt} + \nabla \cdot (\varphi \vec{u}) = 0 \tag{8}$$

where $\vec{u} = (u_z, u_r)$ is the velocity vector. The function φ is defined as $\varphi = 0$ for the gas phase, $\varphi = 1$ for the liquid phase, and $\varphi = 0.5$ for the interface between liquid and gas.

8. Initially, the tube is completely filled with the liquid.

$$t = 0, \quad 0 \le r \le R, \quad -3R \le z \le 3R, \quad \psi = 1 \tag{9}$$

9. The gas is inducted from the entrance.

$$t > 0, \quad 0 \le r \le \overline{EF}, \quad z = -3R, \quad \psi = 0. \tag{10}$$

3. Numerical Scheme

In this study, the finite difference method is used to discretize the differntial equations shown as (2). The terms, which contain the velocity components u_r and u_z, are replaced with ψ and ω by substituting the stream function ψ and the vorticity function ω in (2).

The stream function ψ is defined as

$$u_r = -\frac{1}{r}\frac{\partial \psi}{\partial z}, \quad u_z = \frac{1}{r}\frac{\partial \psi}{\partial r} \tag{11}$$

And the vorticity ω is defined as:

$$\omega = \nabla \times \vec{\mathrm{V}} = -\frac{1}{r}\left(\frac{\partial^2 \psi}{\partial r^2} + \frac{\partial^2 \psi}{\partial z^2} - \frac{1}{r}\frac{\partial \psi}{\partial r}\right) \tag{12}$$

A uniform grid with grid points $(z_i, r_j) = (z_0 + i\triangle z, r_0 + j\triangle r)$ is applied to the discretized system. After repeated testing, the most appropriate resolution is 100 × 600 grid points.

The finite difference formulas are obtained from the terms discretized by FDM with SOR method mentioned above. The differential terms of the stream function and the vorticity function are discretized by a second order central difference method. The velocity of grids is calculated from the stream function by a forward difference method. The discretized system could be shown as [8]:

$$\omega_{i,j}^{K+1} = \frac{\alpha}{\mathrm{e}}\left(\mathrm{a}\omega_{i+1,j}^{K} + \mathrm{b}\omega_{i,j+1}^{K} + \mathrm{c}\omega_{i-1,j}^{K+1} + \mathrm{d}\omega_{i,j-1}^{K+1} + \mathrm{f}\omega_{i,j}^{K}\right) + (1-\alpha)\omega_{i,j}^{K} \tag{13}$$

where

$$\mathrm{a} = \frac{1}{\triangle \mathrm{z}^2} - \mathrm{Re}\frac{\partial \psi^{K}}{\partial r}\frac{1}{\mathrm{r}_0}\frac{1}{2\triangle \mathrm{z}}$$

$$\mathrm{b} = \frac{1}{\triangle \mathrm{r}^2} + \left(1 + \mathrm{Re}\frac{\partial \psi^{K}}{\partial z}\right)\frac{1}{\mathrm{r}_0}\frac{1}{2\triangle \mathrm{r}}$$

$$\mathrm{c} = \frac{1}{\triangle \mathrm{z}^2} + \mathrm{Re}\frac{\partial \psi^{K}}{\partial r}\frac{1}{\mathrm{r}_0}\frac{1}{2\triangle \mathrm{z}}$$

$$\mathrm{d} = \frac{1}{\triangle \mathrm{r}^2} - \left(1 + \mathrm{Re}\frac{\partial \psi^{K}}{\partial z}\right)\frac{1}{\mathrm{r}_0}\frac{1}{2\triangle \mathrm{r}}$$

$$\mathrm{e} = \frac{2}{\triangle \mathrm{z}^2} + \frac{2}{\triangle \mathrm{r}^2} + \frac{1}{(\mathrm{r}_0)^2}$$

$$\mathrm{f} = -\mathrm{Re}\frac{\partial \psi^{K}}{\partial z}\frac{1}{(\mathrm{r}_0)^2}$$

$$\begin{cases} \dfrac{\partial \psi^{K}}{\partial z} = \dfrac{\psi_{i+1,j}^{K} - \psi_{i,j}^{K}}{\triangle \mathrm{z}} \\ \dfrac{\partial \psi^{K}}{\partial r} = \dfrac{\psi_{i,j+1}^{K} - \psi_{i,j}^{K}}{\triangle \mathrm{r}} \end{cases}$$

$$\psi_{i,j}^{K+1} = \frac{\alpha}{\mathrm{e}_1}\left(\mathrm{a}_1\psi_{i+1,j}^{K} + \mathrm{b}_1\psi_{i,j+1}^{K} + \mathrm{c}_1\psi_{i-1,j}^{K+1} + \mathrm{d}_1\psi_{i,j-1}^{K+1} + r\big|_j\,\omega_{i,j}^{K+1}\right) + (1-\alpha)\psi_{i,j}^{*K} \tag{14}$$

where

$$\mathrm{a}_1 = \frac{1}{\triangle \mathrm{z}^2}, \quad \mathrm{b}_1 = \frac{2 - \triangle \mathrm{r} \big/ \mathrm{r}_0}{2\triangle \mathrm{r}^2},$$

$$\mathrm{c}_1 = \frac{1}{\triangle \mathrm{z}^2}, \quad \mathrm{d}_1 = \frac{2 + \triangle \mathrm{r} \big/ \mathrm{r}_0}{2\triangle \mathrm{r}^2}$$

$$\mathrm{e}_1 = \frac{2}{\triangle \mathrm{z}^2} + \frac{2}{\triangle \mathrm{r}^2}$$

where α is the over-relaxation factor. k is the iterative index. i and j are the indices along z-direction and r-direction respectively. $\triangle z$ and $\triangle r$ are the grid sizes along z-direction and r-direction respectively.

Equations (13) and (14) could be solved numerically. The value of the over-relaxation factor α is 1.5 for Re = 0. The value of α is adjusted from 0.5 to 0.025 as Re increases from 10 to 400. The values of ω and ψ are calculated iteratively with an over-relaxation factor α until the converge criterion shown as (15) is reached for some specified ratio ε_ψ

$$\left|\frac{\psi_{i,j}^{k+1}-\psi_{i,j}^{k}}{\psi_{i,j}^{k}}\right| \le \varepsilon_\psi \tag{15}$$

III. INTERFACE TRACKING SCHEME

The evolution of the interface is expressed in the conservation form of the level set function shown in (8). The evolution of the interface is performed by the conservative level set method [14].

As the uniform grid (z_i, r_j) mentioned previously, the grid function is defined as $\varphi_{i,j} = \varphi(z_i, r_j)$. The value of $\varphi_{i,j}$ is ranged from 0 to 1: $\varphi_{i,j} = 0$ for the gas phase, $\varphi_{i,j} = 1$ for the liquid phase, and $\varphi_{i,j} = 0.5$ for the interface between liquid and gas.

The interface is adverted by a given velocity field $\vec{u}$ = (u_r, u_z) obtained from (11) by a first order forward difference method. The discretized equation of (8) with a uniform grid (z_i, r_j) can be written as

$$\frac{\varphi_{i,j}^{k+1}-\varphi_{i,j}^{k}}{\triangle t} = -\frac{1}{\Delta z}\left(F_{i+\frac{1}{2},j}-F_{i-\frac{1}{2},j}\right)-\frac{1}{\Delta r}\left(G_{i,j+\frac{1}{2}}-G_{i,j-\frac{1}{2}}\right) \tag{16}$$

where Δt is the time step, and $\varphi_{i,j}^{k} = \varphi(z_i, r_j)$ at the time step k.

The flux on the grid (z_i, r_j) is represented as:

$$F_{i+\frac{1}{2},j} = 0.5\left(\varphi_{i,j}+\varphi_{i+1,j}\right)u_{i+\frac{1}{2},j} \tag{17}$$

$$G_{i,j+\frac{1}{2}} = 0.5\left(\varphi_{i,j}+\varphi_{i,j+1}\right)v_{i,j+\frac{1}{2}} \tag{18}$$

The velocity on the grid (z_i, r_j) is represented as

$$u_{i+\frac{1}{2},j} = u_r, \text{ and } v_{i,j+\frac{1}{2}} = u_z \tag{19}$$

The normals of the interface can be obtained as

$$\hat{n}_{i,j} = \frac{(\nabla\varphi)_{i,j}}{\left|(\nabla\varphi)_{i,j}\right|} \tag{20}$$

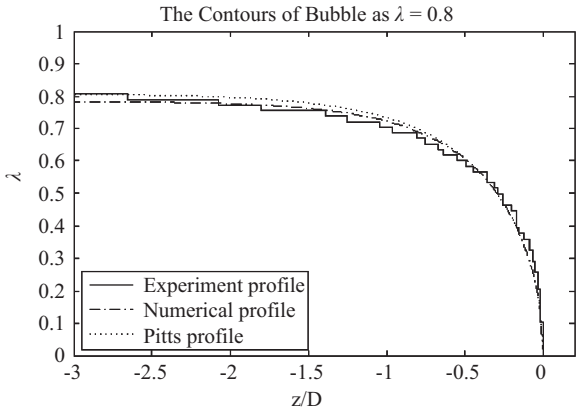

Fig. 2. The comparison of bubble contours by experiment observation, numerical simulation and Pitts equation (λ = 0.8).

The values of φ run smoothly from zero to one on the neighboring interface. The values of $\varphi_{i,j}$ may fill up with either 0 or 1 except the neighboring interface, which is treated as a transition layer or a narrow-band in finite terms to assure the high efficiency performance.

An adaptive strategy is applied to determine the values of time step Δt in order to avoid the value of $\varphi_{i,j}$ being less than 0 or greater than 1. The values of $\Delta t \cdot F_{i+\frac{1}{2},j}$, $\Delta t \cdot F_{i-\frac{1}{2},j}$, $\Delta t \cdot G_{i,j+\frac{1}{2}}$, and $\Delta t \cdot G_{i,j+\frac{1}{2}}$ are controlled under the range between 0.2 and 0.4 by some numerical tests. The values of φ are calculated iteratively till the steady-state criterion shown in (21) is reached

$$\int\left|\varphi^{k+1}-\varphi^{k}\right| \le \varepsilon_\varphi \cdot \Delta t \tag{21}$$

for some specified tolerance ε_φ.

IV. RESULTS AND DISCUSSION

The shape profile equation proposed by Saffman & Taylor agrees very well with the bubble profile obtained by experimental observation only when λ = 0.5 [18]. The modified shape equation proposed by Pitts also agrees with only when λ = 0.54, 0.67, 0.77 [16].

The comparison of bubble contours by experiment observation, numerical simulation and Pitts equation as λ = 0.8 is shown in Fig. 2. The contour plotted in solid line is the bubble profile observed experimently from [9]. The contour plotted in dashed line is the bubble profile obtained by numerical simulation (level set method). The contour plotted in dots is the profile generated by Pitts formula.

The error of the inspected contour is defined as

$$\text{Error} = \frac{\int\left|\lambda-\lambda_{\text{exp}}\right|}{\int\left|\lambda_{\text{exp}}\right|} \tag{22}$$

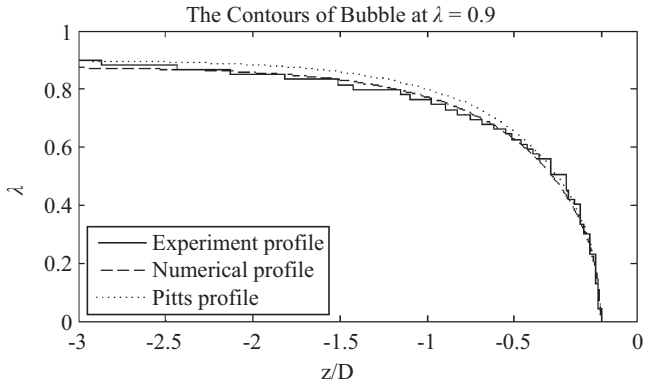

Fig. 3. The comparison of bubble contours by experiment observation, numerical simulation and Pitts equation (λ = 0.9).

where λ is the ratio of the inspected profile diameter to the diameter of the tube. λ_{exp} is the ratio of the experimental profile diameter to the diameter of the tube.

The contour of Pitts profile is very close to the experimental profile at the rear of the asymptotic bubble profile. But it overshoots at the front of the asymptotic bubble profile. The radius of the numerical simulation contour is smaller than that of the experimental profile at the rear of the asymptotic bubble profile. And it is very close to the experimental profile at the front of the asymptotic bubble profile. The difference of both the numerical simulation profile and Pitts profile is about 3%.

Figure 3 shows that the differences of the numerical simulation profile and Pitts profile are 2.5% and 4.6% as λ = 08, 0.9, respectively. The Pitts bubble profile equation is not very accurate as $\lambda > 0.8$. It meets the result of the Pitts' study [16]. However, the numerical simulation contour maintains a stable level even as λ = 0.9.

Since Taylor suggested three flow patterns in front of the bubble in 1961 [21], many researchers have found similar results by experiement and numerical simulation. In 1964, Cox [3] verified the existence of the two flow patterns in [21], and confirmed that the velocity distribution in the viscous fluid was simply the Poiseuille flow at a distance more than 1.5 times the inner diameter of the tube in front of the bubble tip. In 1997, Giavedoni and Saita [6] reported that the stagnation point is located on the center-line between the upstream and the bubble tip in the transient flow pattern. Polynkin *et al.* [17] presented the flow pattern ahead of the gas bubble and the transition criterion between by-pass and recirculating flow using the finite element method in 2005.

Hsu *et al.* [8] showed the ranges of the three flow patterns where the complete bypass flow appears as $\lambda \leqq 0.7071$, the transient flow pattern appears as $0.7071 \leqq \lambda \leqq 0.715$, and the recirculation flow pattern occurs as $\lambda \geqq 0.715$ by the finite difference method in 2005.

Three flow patterns with various λ value are shown in Fig. 4. The flow patterns are determined by the distribution of streamline and vorticity. The stream lines closed to the length of z = 3R are all parallel to each other. It fits the characteristic of

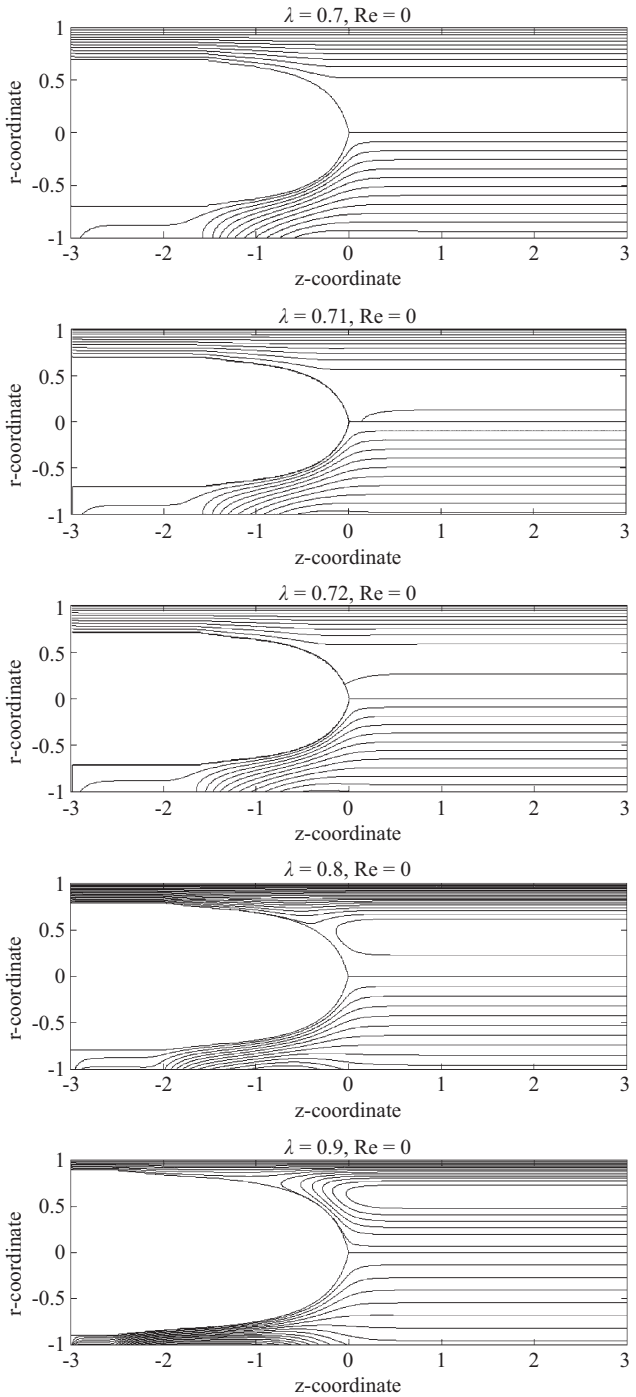

Fig. 4. The contours of the bubble front and the distribution of streamline and vorticity for λ = 0.7, 0.71, 0.72, 0.8, 0.9.

Poiseuille flow [3].

The complete bypass flow appears as λ = 0.7. And the transient flow pattern, which stagnation point is located on the center-line between the upstream and the bubble tip, appears as λ = 0.71. It is consistents with the study of Giavedoni and Saita [9]. Figure 4 also indicates that the recirculation flow pattern, which stagnation point is located on the bubble con-

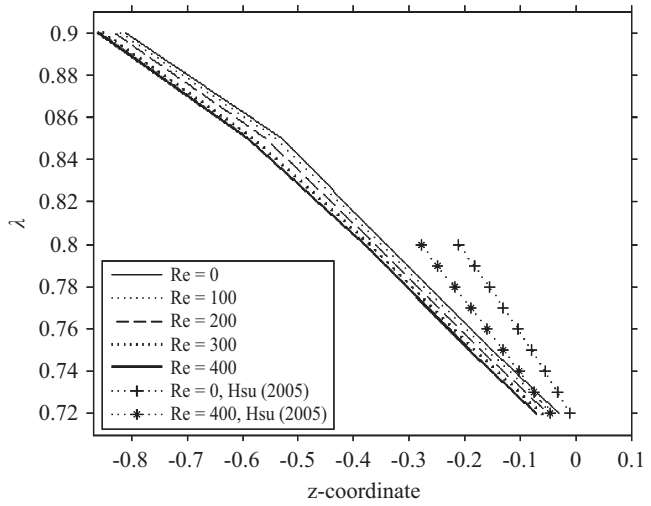

Fig. 5. The relations of the location of the stagnation, λ and Re in the recirculation flow region.

tour, appears as $\lambda \geqq 0.72$. It is consistent with the result of Hsu *et al.* [8].

The relation of the location of the stagnation point z_{sp} and λ with respect to different Reynolds number is shown in Fig. 5. The value of z_{sp} decreases when the value of λ or the Reynolds number increases. The stagnation point moves downstream as λ increases linearly in the range of $0.72 \leqq \lambda \leqq 0.9$ with fixed Reynolds number. The stagnation point also moves downstream as Reynolds number increases linearly in the range of $0 \leqq \text{Re} \leqq 400$ with fixed λ. As Reynolds number increasing from 0 to 400, the difference of z_{sp} is 0.02 and 0.05 with fixed $\lambda = 0.72$ and $\lambda = 0.9$, respectively.

The curve with "+" denoting the location of the stagnation point z_{sp} as Re = 0, and the curve with "*" denoting that for Re = 400, are borrowed from the study of Hsu *et al.* [8]. As Reynolds number increasing from 0 to 400, the difference of z_{sp} is 0.03 and 0.06 with fixed $\lambda = 0.72$ and $\lambda = 0.8$, respectively.

The result is plotted in a slender band with a more gentle slope compared to the result of [8] for the differences in the bubble contours generated by Pitts and the Level Set Method. Even the difference causing by the different bubble profile, yet the same tendency keeps in Fig. 5.

V. CONCLUSION

In this paper, we have studied the penetration of a long bubble through a Newtonian fluid in a horizontal circular tube by numerical simulation. We simulated the evolution of the asymptotic bubble profiles with the interface-tracking method by the conservative level set method. The numerical simulation contour fits the experimental profile very well and stably even as $\lambda = 0.9$.

The type of the flow patterns was correlative to the ratio of asymptotic bubble width to the radius of the circular tube. Three flow patterns suggested by Taylor in front of the bubble, namely the complete bypass flow, the transient flow and the recirculation flow are shown graphically. They all make a good agreement with the study of Giavedoni and Hsu, respectively.

The location of the stagnation point z_{sp} is obviously also correlated with λ. The stagnation point moves downstream as λ increases. A linear character between z_{sp} and λ is revealed as $0.72 \leqq \lambda \leqq 0.9$. The stagnation point moves downstream with an almost constant rate of λ in the range of $0.72 \leqq \lambda \leqq 0.9$ and $0 \leqq \text{Re} \leqq 400$.

REFERENCES

1. Adalsteinsson, D. and Sethian, J. A., "A fast level set method for propagating interfaces," *Journal of Computational Physics*, Vol. 118, pp. 269-277 (1995).
2. Bonometti, T. and Magnaudet, J., "An interface-capturing method for incompressible two-phase flows. Validation and application to bubble dynamics," *International Journal of Multiphase Flow*, Vol. 33, pp. 109-133 (2007).
3. Cox, B. G., "An experimental investigation of the streamlines in viscous fluids expelled from a tube," *Journal of Fluid Mechanics*, Vol. 20, pp. 193-200 (1964).
4. Fukagata, K., Kasagi, N., Ua-arayaporn, P., and Himeno, T., "Numerical simulation of gas-liquid two-phase flow and convective heat transfer in a micro tube," *International Journal of Heat and Fluid Flow*, Vol. 28, pp. 72-82 (2007).
5. Gauri, V. and Koelling, K. W., "Gas-assisted displacement of viscoelastic fluids: Flow dynamics at the bubble front," *Journal of Non-Newtonian Fluid Mechanics*, Vol. 83, pp. 183-203 (1999).
6. Giavedoni, M. D. and Saita, F. A., "The axisymmetric and plane cases of a gas phase steadily displacing a Newtonian liquid: A simultaneous solution of the governing equations," *Physics of Fluids*, Vol. 9, pp. 2420-2428 (1997).
7. Hirt, C. W. and Nichols, B. D., "Volume of fluid (VOF) method for the dynamics of free boundaries," *Journal of Computational Physics*, Vol. 39, pp. 201-225 (1981).
8. Hsu, C.-H., Chen, P.-C., Kung, K.-Y., and Lai, C., "Impacts of ratio of asymptotic bubble width to diameter of circular tube and Reynolds number in a gas bubble driven flow," *Chemical Engineering Science*, Vol. 60, pp. 5341-5355 (2005).
9. Hsu, C.-H., Kung, K.-Y., Chen, P.-C., and Hu, S.-Y., "Experimental visualization of gas-assisted injection long bubble in a tube," *WSEAS Transactions on Applied and Theoretical Mechanics*, Vol. 4, pp. 1-10 (2009).
10. Huzyak, P. C. and Koelling, K. W., "The penetration of a long bubble through a viscoelastic fluid in a tube," *Journal of Non-Newtonian Fluid Mechanics*, Vol. 71, pp. 73-88 (1997).
11. Kamisli, F., "Gas-assisted displacement of a viscoelastic fluid in capillary geometries," *Chemical Engineering Science*, Vol. 61, pp. 1203-1216 (2006).
12. Losasso, F., Fedkiw, R., and Osher, S., "Spatially adaptive techniques for level set methods and incompressible flow," *Computers & Fluids*, Vol. 35, pp. 995-1010 (2006).
13. Nagrath, S., Jansen, K. E., and Lahey, R. T., Jr., "Computation of incompressible bubble dynamics with a stabilized finite element level set method," *Computer Methods in Applied Mechanics and Engineering*, Vol. 194, pp. 4565-4587 (2005).
14. Olsson, E. and Kreiss, G., "A conservative level set method for two phase flow," *Journal of Computational Physics*, Vol. 210, pp. 225-246 (2005).
15. Osher, S. and Sethian, J. A., "Fronts propagating with curvature-dependent speed: Algorithms based on Hamilton-Jacobi formulations," *Journal of Computational Physics*, Vol. 79, pp. 12-49 (1988).
16. Pitts, E., "Penetration of gluid into a Hele-Shaw cell: The Saffman-Taylor experiment," *Journal of Fluid Mechanics*, Vol. 97, pp. 53-64 (1980).

17. Polynkin, A., Pittman, J. F. T., and Sienz, J., "Gas displacing liquids from non-circular tubes: High capillary number flow of a shear-thinning liquid," *Chemical Engineering Science*, Vol. 60, pp. 1591-1602 (2005).
18. Saffman, P. G. and Taylor, G. I., "The penetration of a fluid into a porous medium or Hele-Shaw cell containing a more viscous liquid," *Proceedings of the Royal Society of London, Series A*, Vol. 245, pp. 312-329 (1958).
19. Sethian, J. A., "Evolution, implementation, and application of level set and fast marching methods for advancing fronts," *Journal of Computational Physics*, Vol. 169, pp. 503-555 (2001).
20. Sussman, M. and Puckett, E. G., "A coupled level set and volume-of-fluid method for computing 3D and axisymmetric incompressible two-phase Flows," *Journal of Computational Physics*, Vol. 162, pp. 301-337 (2000).
21. Taylor, G. I., "Deposition of a viscous fluid on the wall of a tube," *Journal of Fluid Mechanics*, Vol. 10, pp. 161-165 (1961).
22. Tomiyama, A., Zun, I., Sou, A., and Sakaguchi, T., "Numerical analysis of bubble motion with the VOF method," *Nuclear Engineering and Design*, Vol. 141, pp. 69-82 (1993).
23. Zhong, W., Zhang, M., Jin, B., and Chen, X., "Flow pattern and transition of rectangular spout-fluid bed," *Chemical Engineering and Processing*, Vol. 45, pp. 734-746 (2006).